FULL PAPER

PPS www.rsc.org/pps

Excited-state dynamics of the fluorescent probe Lucifer Yellow in liquid solutions and in heterogeneous media

Alexandre Fürstenberg and Eric Vauthey*

Department of Physical Chemistry, University of Geneva, 30 Quai Ernest-Ansermet, 1211, Genève 4, Switzerland. E-mail: eric.vauthey@chiphy.unige.ch; Fax: +41 22 3796518; Tel: +41 22 3796804

Received 2nd December 2004, Accepted 13th January 2005
First published as an Advance Article on the web 3rd February 2005

The photophysics of the dye Lucifer Yellow ethylenediamine (LYen) has been investigated in various polar solvents. The main deactivation pathways of its first singlet excited state are the fluorescence and the intersystem crossing. In water, non-radiative decay by intermolecular proton transfer becomes a significant deactivation channel. The early fluorescence dynamics, which was investigated in liquids and in reverse micelles, was found to depend substantially on the environment. An important static quenching of LYen by tryptophan and indole occurring in the subpicosecond timescale was observed. The use of the fluorescence dynamics of LYen as a local probe is illustrated by preliminary results obtained with a biotinylated Lucifer Yellow derivative complexed with avidin.

Introduction

Since their introduction about 25 years ago, Lucifer Yellow derivatives have found large application in biological tracing.[1,2] Apart from their widespread use as tools for studying neuronal morphology[1,3–5] and function,[6,7] they have also served as cytoplasmic or endosomal markers,[8,9] reactive labels for tissue staining,[10,11] tracers in confocal or electron microscopy,[2,12–14] protein labelling agents,[15–17] and tracers of cell-cell fusion, membrane permeability, or cell uptake.[18–20] These dyes are based on a sulfonated 4-amino-1,8-naphthalimide moiety with a variable substituent on the imide nitrogen. Good water solubility, quantum yields of the order of 0.25, wide spectral separation of absorption and emission maxima (430 and 530 nm, respectively) make Lucifer Yellow salts readily visible in living cells at concentrations and levels of illumination at which they are non-toxic. Aqueous solutions of these dyes appear further to be chemically stable for at least several months at room temperature.

Although the excited-state properties of several naphthalimide derivatives have been investigated in detail,[21–28] relatively little is known about those of Lucifer Yellow. Its fluorescence steady-state spectrum and lifetime have been shown to be environment-sensitive,[17,29,30] but these studies were not systematic. Moreover, ultrafast processes following the optical excitation of a dye, such as vibrational cooling,[31–33] dynamic Stokes shift,[34,35] and fluorescence depolarisation[36,37] have been shown to be environment-dependent, but the ultrafast fluorescence dynamics of Lucifer Yellow is totally unknown. Furthermore, proteins are often tagged with Lucifer Yellow, but the spectral properties and the fluorescence quantum yield may be modulated by nearby protein residues as suggested by recent observations.[17]

We report here on our investigation of the photophysical properties of Lucifer Yellow ethylenediamine (LYen)† in various solvents using both steady-state and time-resolved techniques. The aim of this study was first to understand the basic excited-state properties of this dye and second to explore its ultrafast fluorescence dynamics in order to establish its potential use as an environment-sensitive probe, especially in aqueous media. An investigation of the fluorescence quenching of LYen by various electron donors is presented as well. To illustrate a possible application of this dye as local probe, a preliminary study with the commercial construct Lucifer Yellow biocytin (LYbtn, Scheme 1), in which the dye is coupled to D-biotin *via* a 13-atom spacer, in the local environment of avidin is described.

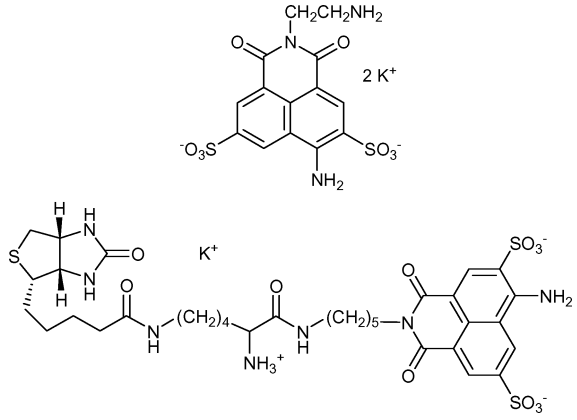

Scheme 1 Molecular structure of the dyes LYen (top) and LYbtn (bottom).

Experimental

Samples

LYen and LYbtn were purchased from Molecular Probes, methanol, tryptophan (Trp) and indole (Ind) from Fluka, DMSO, DMF, rhodamine 6G (R6G), aerosol OT (AOT), and *n*-heptane from Acros Organics. All compounds were of the highest commercially available grade and used without further purification. Avidin was a gift of Professor Thomas R. Ward (University of Neuchâtel, Switzerland). 500 μM stock solutions of LYen in water, DMF, and DMSO were prepared and stored in the dark. LYbtn (1 mM in DMSO) and avidin (100 μM in

† Abbreviations are: AOT, dioctyl sulfosuccinate sodium salt (aerosol OT); DMF, *N*,*N*-dimethylformamide; DMSO, dimethylsulfoxide; ESPT, excited-state proton transfer; ET, electron transfer; FWHM, full width at half maximum; Ind, indole; ISC, intersystem crossing; LYbtn, Lucifer Yellow biocytin potassium salt (biocytin: ε-*N*-(D-biotinyl)-L-lysine); LYen, Lucifer Yellow ethylenediamine dipotassium salt (*N*-(2-aminoethyl)-4-amino-3,6-disulfo-1,8-naphthalimide dipotassium salt); R6G, rhodamine 6G; TCSPC, time-correlated single photon counting; Trp, L-tryptophan.

DOI: 10.1039/b418188c

bidistilled water) stock solutions were stored at −20 °C. All samples were freshly prepared from these solutions. Typical dye concentrations for steady-state and time-correlated single photon counting (TCSPC) measurements were 1–10 μM and *ca.* 100–200 μM in up-conversion experiments.

Reverse micelle-containing samples were prepared by mixing in the sample cell adequate volumes of a stock solution of 0.1 M AOT in *n*-heptane (1 M for up-conversion measurements) with a 490 μM stock solution of LYen in water. Solutions were shaken by hand and micelles formed instantaneously. Micelles were assumed to be spherical and their inner radius *r* (Å) was calculated with the relationship[38]

$$r = 1.5\ R \tag{1}$$

where *R* is the water to surfactant molar ratio. In quenching experiments, 40 mM Trp in water and 30 mM Trp in DMSO stock solutions were prepared and diluted to the working concentrations (LYen concentration: 1.5 μM) for steady-state and TCSPC measurements. In up-conversion experiments, desired amounts of Trp were directly dissolved in 200 μM LYen solutions.

All samples were purged with nitrogen or argon before the measurements. No significant degradation of the samples was observed after the measurements.

Steady-state measurements

Absorption spectra were recorded on a Cary 50 spectrophotometer and fluorescence spectra on a Cary Eclipse fluorimeter using 1 cm quartz cells.

The fluorescence quantum yield of LYen in water, DMF, and DMSO was determined against R6G, whose quantum yield was taken as 0.89.[39]

Time-resolved fluorescence measurements

Excited-state lifetime measurements in the nanosecond time scale were done with the time-correlated single photon counting (TCSPC) technique. Excitation was performed at 395 nm with a pulsed laser diode (Picoquant model LDH-P-C-400B). The pulses had a duration of about 65 ps and the average power was about 0.5 mW at 20 MHz. Fluorescence was collected at 90°, and passed through an analyzer set at the magic angle with respect to the excitation polarization, and a 420 nm-cut-off filter located in front of a photomultiplier tube (Hamamatsu, H5783-P-01). The detector output was connected to the input of a TCSPC computer board module (Becker and Hickl, SPC-300-12). The full width at half maximum (FWHM) of the instrument response was around 200 ps. Measurements were performed in a 1 cm quartz cell. The accuracy on the lifetimes is of *ca.* 0.1 ns.

The fluorescence up-conversion set-up has already been described elsewhere.[40] Briefly, the frequency-doubled output of a Kerr lens mode-locked Ti:sapphire laser (Tsunami, Spectra-Physics) was used for excitation of the sample at 400 nm. The output pulses centred at 800 nm had a duration of 100 fs and a repetition rate of 82 MHz. The pump intensity on the sample was around 10^{14} photons cm^{-2} $pulse^{-1}$. The polarization of the pump beam was at magic angle relative to that of the gate pulses at 800 nm except for fluorescence anisotropy measurements. Experiments were carried out in a 0.4 or 1 mm rotating cell with an absorbance of *ca.* 0.1 at 400 nm to avoid reabsorption. The FWHM of the instrument response function was *ca.* 240 fs with a 0.4 mm cell and 280 fs with a 1 mm cell.

Fluorescence anisotropy measurements on the nanosecond time scale were done with the TCSPC set-up. For each sample, two fluorescence traces were recorded, one with the analyzer set parallel to the excitation beam polarization ($I_{para}(t)$), the second with the analyzer set perpendicularly ($I_{perp}(t)$). Anisotropy decays $r(t)$ were then reconstructed using the standard equation

$$r(t) = \frac{I_{para}(t) - I_{perp}(t)}{I_{para}(t) + 2I_{perp}(t)} \tag{2}$$

Femtosecond-resolved fluorescence anisotropy measurements were carried out with the up-conversion set-up by changing the polarization of the pump beam with respect to the probe beam by rotating a Berek plate and monitoring the fluorescence kinetics at 550 nm. The anisotropy was reconstructed as described above.

Fluorescence data analysis

Time-resolved fluorescence data were analysed by iterative reconvolution of the instrument response function with trial functions (sum of exponentials) using a non-linear least-squares fitting procedure (MATLAB, The MathWorks, Inc.). Measurements were carried out at 6 to 10 different wavelengths from 450 up to 640 nm for the LYen-containing samples. In most cases, measurements were performed over three time scales, to accurately cover the span of the fluorescence decay. Before analyzing the data globally, the raw kinetics were first corrected for residual fluorescence due to excitation by the previous light pulse by simple subtraction (the residual fluorescence intensity can be estimated as constant on the investigated time scales), and then rescaled. The rescaling factor, $F(\lambda)$, was obtained from the following ratio

$$F(\lambda) = \frac{S(\lambda)}{\int_0^\infty D(\lambda, t)dt} \tag{3}$$

where $D(\lambda,t)$ is the time profile of the fluorescence intensity and $S(\lambda)$ is the steady state fluorescence intensity.

The accuracy on the lifetimes and on the amplitudes obtained by this method is estimated to *ca.* 10%, except on lifetimes shorter than about 500 fs (uncertainty of about 200 fs).

Transient absorption experiments

Microsecond transient absorption measurements were performed using a conventional laser flash photolysis set-up. Excitation was achieved at 355 nm with the frequency-tripled output of a Q-switched active-passive mode-locked and cavity dumped Nd:YAG laser (pulse duration: 25 ps; repetition rate: 10 Hz; pulse energy: 5 mJ). The sample was held in a 1 cm quartz cuvette and had a typical absorbance of 0.25 at 355 nm. The output of a continuous Hg–Xe lamp (Hamamatsu model E7536) was used for probing. The data acquisition was made with a 500 MHz digital oscilloscope (Tektronix TDS 620A).

For ultrafast transient absorption experiments, excitation was achieved at 400 nm with the frequency-doubled output of a standard 1 kHz amplified Ti:sapphire system (Spitfire, Spectra-Physics). The duration of the pulses at 400 nm was around 120 fs. For probing, a home-built non-colinear optical parametrical amplifier, generating pulses tunable between 480 and 700 nm, was used.[41] For the experiments reported here, the probe wavelength was set at 580 nm and the pulse duration was 50 fs. The FWHM of the instrument response function was around 200 fs. Detection was achieved at the magic angle. The sample solutions were placed in a 1 mm quartz cell, had an absorbance of 0.4 (LYen 500 μM and Trp 40 mM) and were stirred by N_2 bubbling.

Results and discussion

Steady-state and nanosecond photophysics

The choice of solvents in which LYen can be investigated is rather reduced. Indeed, this dye was found to be only readily soluble in water, DMF, and DMSO, but not in alcohols. The poor solubility in alcohols might be due to the use of a potassium salt of the ethylenediamine derivative of Lucifer Yellow whereas other groups worked with a lithium salt of the carbohydrazine

derivative.[29] Steady-state absorption and fluorescence spectra (Fig. 1) exhibit a single and broad band characteristic of a charge transfer transition and a large Stokes shift, which increases with solvent polarity from about 3600 cm^{-1} in DMF to about 4300 cm^{-1} in water. Interestingly, the absorption band is shifted to the blue and the fluorescence spectrum to the red with increasing solvent polarity, and especially when going from aprotic to protic solvents. H-bonding in both ground and excited states but at different positions is known to lead to a blue and a red shift of the absorption and emission bands, respectively, when going from an aprotic to a protic solvent.[42] This anomalous solvatochromism might as well be related to the eccentricity of the position of the ground state dipole moment.[42,43] The ground state dipole moment is determined by groups relatively far from the centre of the molecule and this leads to an increase of the effective Onsager reaction field in the dipole position and thus of the ground state solvation energy. On the other hand, the fluorescent state of 4-aminonaphthalimide derivatives is known to have a relatively strong charge transfer character, and the corresponding electric dipole moment can be reasonably well approximated to a point dipole located in the centre of the cavity. This situation is predicted to lead to a blue shift of the absorption band and to a red shift of the fluorescence spectrum.[43] Independently on the origin of this effect, it can be safely concluded that the excited-state dipole moment of LYen is considerably larger than that of its ground state.

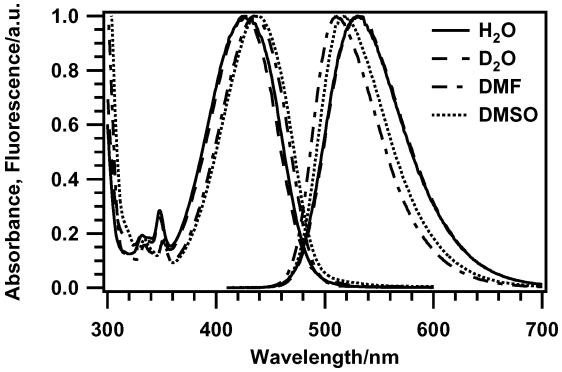

Fig. 1 Normalized steady-state absorption and fluorescence spectra of LYen in water, deuterium oxide, DMF, and DMSO. Excitation occurred at 400 nm.

The quantum yield was determined against R6G and was found to be 0.27 in water, which is in agreement with literature values,[2,17] 0.53 in deuterium oxide, and around 0.7 in DMF and DMSO (Table 1). Excited-state (S_1) lifetimes were determined using the TCSPC technique. The fluorescence decays could be very well reproduced with a single exponential function (Fig. 2) with a lifetime of 5.7 ns in H_2O, 10.6 ns in DMSO, 11.3 ns in DMF, and 11.5 ns in D_2O. As already suggested by Lee and Fortes,[29] this variation of the excited-state lifetime is consistent with that measured with the fluorescence quantum yield. Indeed, the values obtained by multiplying the radiative lifetime by the cube of the refractive index[44] are essentially the same for all four solvents.

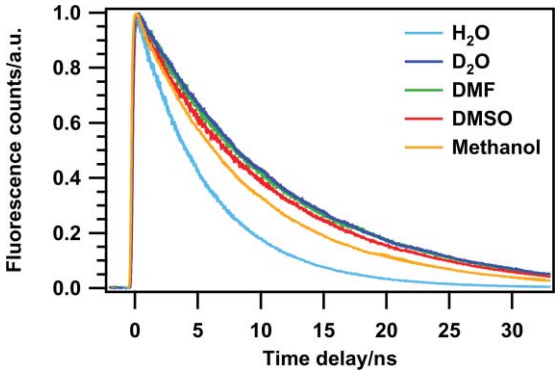

Fig. 2 Fluorescence decays of LYen in water, deuterium oxide, DMSO, DMF, and methanol, reproduced with a single exponential function (solid line).

The significantly lower excited-state lifetime and fluorescence quantum yield of LYen in H_2O, as compared to the other solvents, is not due to a more efficient population of the triplet state in H_2O as microsecond transient absorption experiments showed (Fig. 3); on the contrary, the relative triplet yield, determined in solutions sharing the same absorbance at 355 nm, was lower in H_2O, which implies that an additional deactivation channel is operative in this solvent. The direct comparison of the TCSPC data obtained in H_2O and D_2O rather suggests this channel being an excited-state proton transfer (ESPT) with the solvent. The charge-transfer, which is believed to take place upon LYen photoexcitation between the amino group of the naphthalene ring and the carbonyl oxygens, is predicted to increase the basicity of the latter atoms; they may subtract a proton from a protic solvent molecule and this finally quenches the excited LYen. The strong increase of fluorescence lifetime when going from H_2O to D_2O strongly supports the occurrence of this process. ESPT is a well-known quenching process of many aromatic ketones[45,46] and has been reported with other aminonaphthalimide derivatives.[25] The ESPT hypothesis is further supported by a TCSPC experiment with a methanol solution in which a drop of LYen in DMSO had been added, which

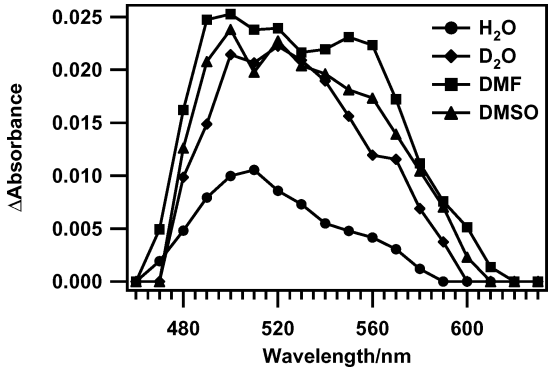

Fig. 3 Transient absorption spectra of the triplet excited state of LYen in different solvents 500 ns after excitation at 355 nm. All samples had the same absorbance of 0.25, so that the absolute values of the signal can be compared directly.

Table 1 Photophysical properties of LYen in different solvents

Solvent	A_{max}/nm[a]	E_{max}/nm[a]	ε_{400}/cm^{-1} M^{-1}[b]	Φ_{fl}[c]	τ_{fl}/ns[d]	τ_{rad}/ns[e]	τ_{ISC}/ns[f]	τ_{ESPT}/ns[g]
H_2O	428	530	7900	0.27	5.7	21.1	24.5[h]	11.5[i]
D_2O	428	528	ND[j]	0.53	11.5	21.7	24.5	
DMSO	439	518	4700	0.68	10.6	15.6	33.1	
DMF	435	510	5700	0.70	11.3	16.1	37.7	

[a] Absorption and emission maxima. Accuracy: ±2 nm. [b] Molar extinction coefficient at 400 nm. Accuracy: ±10%. [c] Quantum yield determined against R6G, whose quantum yield was taken as 0.89.[39] Accuracy: ±10%. [d] Fluorescent-state lifetime. Accuracy: ±0.1 ns. [e] Calculated radiative lifetime, $\tau_{rad} = \tau_{fl}/\Phi_{fl}$. [f] Calculated intersystem crossing time constant. [g] Calculated excited-state proton transfer time constant. [h] Value estimated to be the same as in D_2O. [i] Obtained with a value for τ_{ISC} of 24.5 ns. [j] ND: not determined.

yielded an excited-state lifetime for LYen in methanol of 8.8 ns, a significantly shorter value than in the tested aprotic solvents (Fig. 2). A simple calculation, assuming the only deactivation channels for LYen* being fluorescence, intersystem crossing to the triplet excited state (ISC), and ESPT, and the ESPT rate being negligible in all solvents except H_2O, gives a characteristic time for the proton transfer of 10–12 ns, which is a reasonable time scale for an intermolecular proton transfer.[47,48] Assuming internal conversion to be negligible, the excited-state dynamics of LYen in the nanosecond time scale can thus be summarized as follows (Table 1): LYen* deactivates *via* fluorescence ($\tau_{rad} \approx$ 15–20 ns) and intersystem crossing ($\tau_{ISC} \approx$ 25–35 ns) in aprotic media, and mainly by intermolecular proton transfer ($\tau_{ESPT} \approx$ 10–12 ns) in protic solvents.

Ultrafast dynamics

The ultrafast fluorescence dynamics of LYen in H_2O, DMF, and DMSO was investigated by fluorescence up-conversion and monitored at 6 to 10 different wavelengths spanning most of the fluorescence spectrum (450 to 640 nm). The early dynamics is characterized by decays in the blue part of the spectrum and rises in the red part (Fig. 4). For water and DMF, the data

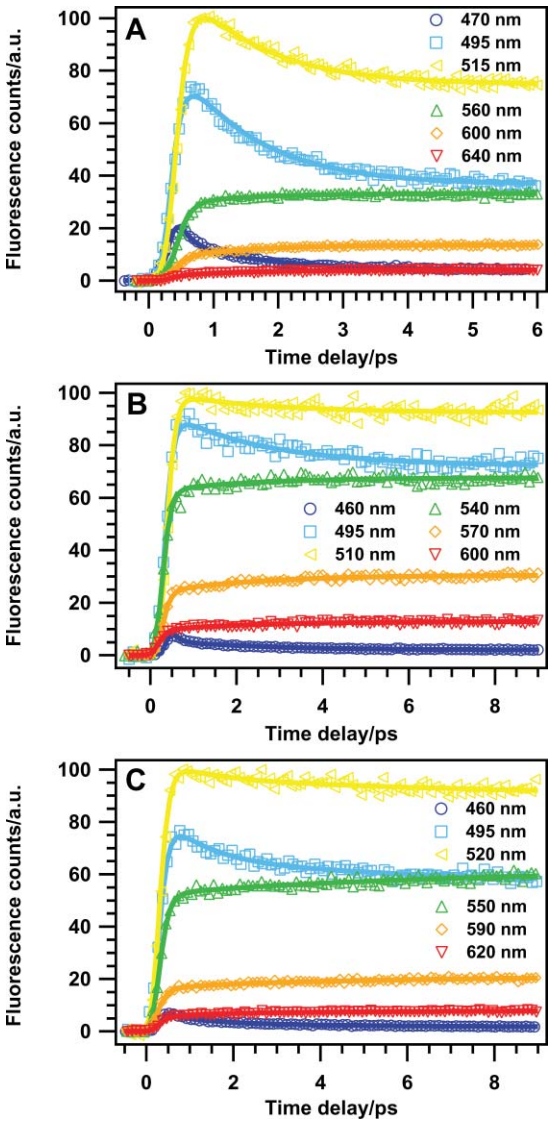

Fig. 4 Fluorescence dynamics of LYen in water (A), DMF (B), and DMSO (C) at different wavelengths upon excitation at 400 nm. Raw data (open circles) were deconvolved with a response function of 240 fs FWHM and globally analysed with three exponential functions (solid lines). The relative intensities were normalized with respect to the steady-state fluorescence intensity at each wavelength.

Table 2 Lifetimes τ_i obtained from the global analysis of the ultrafast fluorescence kinetics of LYen in water, DMF, and DMSO. Accuracy: ±10%. The lifetime of the nanosecond component was fixed to the values measured in the TCSPC experiments

Solvent	τ_1/fs	τ_2/ps	τ_3/ns	τ_4/ps
Water	140	1.2	5.7	—
DMF	110	2.2	11.3	—
DMSO	140	1.0	10.6	8.3

were deconvolved and fitted globally using three exponential functions, two of them reflecting the dynamics on an ultrashort time scale, and the third one fixed to the value of the nanosecond decay obtained through the TCSPC experiments. For both solvents, the fit yielded a lifetime of the order of 100 fs, *i.e.* smaller than the instrument response function (IRF), and another of the order of a few picoseconds (Table 2). The spectral dependence of the amplitude of the nanosecond component (a_3) reflects rather closely the fluorescence steady-state spectrum (data shown only for water, Fig. 5). The amplitude of the ultrashort component is positive in the blue part of the fluorescence spectrum, highly negative in the central part and close to zero on the red side (Fig. 5). This corresponds to a red shift and to a simultaneous narrowing of the fluorescence spectrum. This and the very short time constant suggest the involvement of both vibrational relaxation and inertial solvation.[31,49] The 1–2 ps component exhibits positive amplitudes in the blue side and negative amplitudes in the red and can be associated to a dynamic Stokes shift related to the slower part of solvation in water, *i.e.* the diffusive solvent motion. Similar time constants have been observed with other probe molecules in both water and DMSO.[34,49,50]

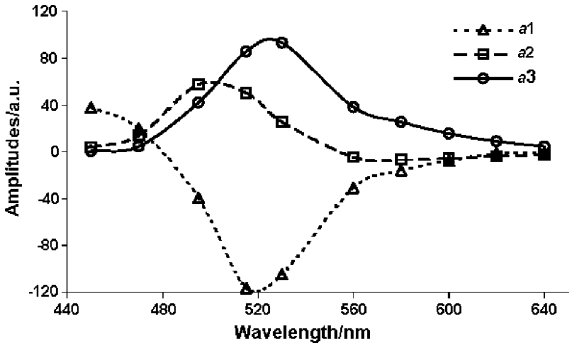

Fig. 5 Amplitudes a_i (corresponding to the τ_i time constants) obtained from the global fit on the ultrafast fluorescence dynamics of LYen in water monitored at different wavelengths.

In DMSO, the early fluorescence dynamics cannot be satisfactorily reproduced with less than three exponential functions. The time constants of the two shortest components are similar to those found in the other two solvents, namely 140 fs and 1.0 ps. The time constant of the additional component is substantially larger and amounts to 8.3 ps. These three time constants are very similar to those reported for the fluorescence Stokes shift of coumarin 153 in DMSO.[34]

To further probe the sensitivity of LYen to its environment, the reorientational dynamics of the dye was measured in *n*-heptane-AOT-water reverse micelles with different water-to-AOT ratios (defined as *R*). For *R* values up to 15, the time-resolved fluorescence anisotropy measurements were performed by TCSPC, but for larger values the up-conversion set-up had to be used, since the anisotropy decay was found to be strongly speeded up with increasing the micelle size (Table 3). In bulk water (Fig. 6) and at an *R* of 20, the decays could be well reproduced with a single exponential function with a time constant of 100 and 140 ps, respectively. In micelles with smaller *R*, the fluorescence anisotropy decay is clearly biphasic with a

Table 3 Amplitudes a_i and characteristic reorientation times $\tau_{rot,i}$ measured for LYen in *n*-heptane–AOT–water reverse micelles with different water-surfactant ratios *R*. Accuracy: ±10%. As an indication, the approximate number of water molecules per micelle, *N*, is given. Spherical micelles were assumed

R	*N*	a_1	$\tau_{rot,1}$/ps	a_2	$\tau_{rot,2}$/ns
1.7	2–3	—	—	1.00	2.6
5.0	≈60	0.43	800	0.57	2.6
10.0	≈470	0.87	480	0.13	2.6
15.0	≈ 1600	0.82	350	0.18	2.6
20.0	≈ 4000	1.00	140	—	—
Bulk	∞	1.00	100	—	—

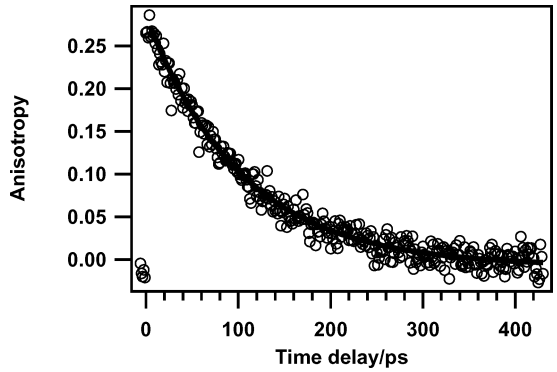

Fig. 6 Time-resolved fluorescence anisotropy of LYen in bulk water. The decay (open circles) was reproduced with a single exponential function (solid line).

slow component apparently independent of *R* and a fast one which slows down with decreasing *R*. This trend was confirmed by a global analysis using a biexponential function. A 2.6 ns component with a relative amplitude increasing with decreasing *R* was found in all decays (see Table 3). On the other hand, the lifetime of the faster component changed from 800 to 350 ps by going from $R = 5$ to 15.

The 2.6 ns component is due to dye molecules with strongly restricted motion, probably because they reside in the palisade layer of the micelle. On the other hand, the fast and *R*-dependent decay component is most probably due to LYen molecules dissolved in the water pool at the interior of the micelles, where reorientational motion is much easier. Micellar water is known to possess particular properties due to the fact that some molecules are bound to the polar head groups of the AOT micelles. Thus, these molecules cannot form the normal hydrogen bonds found in bulk water,[51–53] their mobility is strongly affected,[54] and the water pool becomes heterogeneous with respect to the microviscosity.[55] The slowing down of the fluorescence depolarisation with decreasing *R* indicates an increase of the local viscosity. A similar conclusion has been reported with other microviscosity probes, such as the fluorescence quantum yield and the lifetime of Auramine O.[55] Heterogeneous microenvironments are also expected at biological surfaces and these results suggest that LYen should be able to sense the vicinity of a cell membrane or of a protein. The diversity of water molecules at protein or nucleic acid surfaces has recently been demonstrated by Zewail and co-workers.[56]

Intermolecular quenching studies

Additionally to the processes discussed above, the presence of residues in the close vicinity of a biomolecule marker can also affect its fluorescence dynamics. To test this hypothesis, Trp was chosen as a model compound since the Trp residue is known to be the most readily oxidized functional group among all naturally occurring amino acids.[57,58] Changes in fluorescence intensity and lifetime of LYen in water in the presence of variable Trp concentrations were monitored and analysed in terms of a Stern–Volmer plot (Fig. 7). The decrease of fluorescence lifetime upon addition of Trp was found to be small compared to the strong fall of the steady-state fluorescence intensity, thus suggesting the occurrence of a strong static quenching, probably due to the formation of a ground-state complex between LYen and Trp. This hypothesis is supported by slight distortions of the 430 nm absorption band of LYen in the presence of Trp. Moreover, ground state complex formation between R6G or fluorescein and Trp in water have already been reported.[58] To test whether the effect was due to a coulombic interaction between the charged groups of Trp and LYen or rather to a π–π interaction between the aromatic rings, the same measurements were performed with Ind instead of Trp. Both molecules have a similar oxidation potential,[59] but Ind lacks the polar head groups of Trp. The fluorescence quenching patterns are similar to those observed with Trp, although the magnitude of the static quenching was found to be a little lower, suggesting that the static quenching process mainly arises from a π–π interaction between LYen and Trp or Ind.

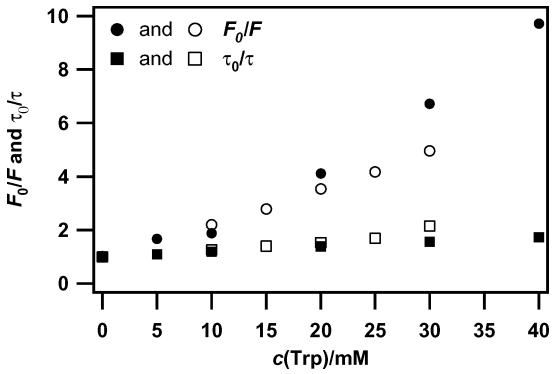

Fig. 7 Static (circles) and dynamic (squares) quenching of LYen by Trp (filled symbols) and Ind (open symbols) in water.

From the slope of the Stern–Volmer plots obtained from the lifetimes, rate constants of dynamic quenching of 3.2×10^9 and 4.8×10^9 M^{-1} s^{-1} were found with Trp and Ind, respectively. As the rate constant of diffusion in water is of the order of 6×10^9 M^{-1} s^{-1},[60] it can be concluded that the dynamic quenching process is quite efficient.

The time scale at which the static quenching process occurs was evaluated with Trp using ultrafast time-resolved fluorescence measurements at 550 nm, a wavelength at which the fluorescence decay is expected to be due to population dynamics only. Indeed, without quencher, the time profile of the fluorescence intensity at 550 nm is flat on a picosecond time scale (Fig. 8A). At all investigated Trp concentrations different from zero, an ultrafast component with a time constant of about 720 ± 100 fs was found from a global fit, its amplitude rising with increasing Trp concentration (Table 4). This ultrafast component is present at other detection wavelengths as well (Fig. 8B).

Several studies have revealed that inserted organic dyes readily oxidize DNA, especially guanosine residues, which have the lowest oxidation potential among the bases.[61,62] Since Trp and Ind have even lower oxidation potentials than guanosine (E_{ox}(Trp) = 0.84 V *vs.* SCE,[57,63] E_{ox}(Ind) ≈ E_{ox}(Trp)[59]) it is likely that the quenching of LYen by Trp and Ind also arises from photoinduced electron transfer (ET) from the amino acid to the dye, a coplanar stacking ground state complex conformation which favours electronic coupling being readily conceivable.[64] Such conformation has already been observed between riboflavin and Trp in the crystal structure of the riboflavin–riboflavin-binding protein complex.[65] It also reduces the water accessible area. The lack of this water-hiding driving force could explain why no such static fluorescence quenching of LYen by Ind (Trp was not soluble) was detected in DMSO (data

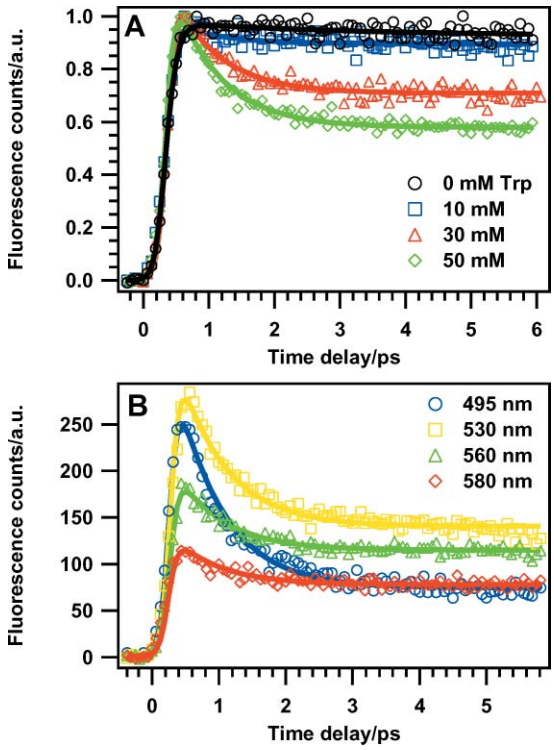

Fig. 8 Fluorescence kinetics of LYen in the presence of Trp upon excitation at 400 nm. Open circles are data points while solid lines result from a global fit over each set of kinetic traces. (A) Fluorescence dynamics at 550 nm of LYen in presence of various Trp concentrations (0–50 mM). (B) Fluorescence dynamics of LYen in the presence of 50 mM Trp at different wavelengths.

Table 4 Parameters obtained from the global analysis done on the fluorescence dynamics of Fig. 8A. The fluorescence lifetimes of the S_1 state τ_{S1} were obtained from TCSPC measurements and fixed during the fit. The lifetime of the ET process, τ_{ET}, was a global parameter. The a_i are the amplitudes of the two components (accuracy: ±10%)

c(Trp)/mM	a_{S1}	τ_{S1}/ns	a_{ET}	τ_{ET}/ps
0	1.00	5.7	—	—
10	0.91	4.8	0.09	0.72 ± 0.10
30	0.64	3.7	0.36	0.72 ± 0.10
50	0.51	3.0	0.49	0.72 ± 0.10

not shown). The reduction potential of LYen is not known, but the presence of the 4-amino group can be expected to reduce considerably the oxidation power of this dye compared to other naphthalimide derivatives, whose reduction potential is of the order of −1 V *vs.* SCE.[66,67] Therefore, the driving force for the photoinduced ET between LYen and Trp should be less negative than −0.5 eV. An ET quenching with such a low driving force is expected to be slower than diffusion, as observed here. On the other hand, a very specific geometry of the ground state complex could account for an ultrafast intracomplex ET. The occurrence of this process is further confirmed by time-resolved absorption measurements at 580 nm, where the tryptophan radical cation $Trp^{\bullet+}$ has been reported to absorb (Fig. 9).[68] Apart from the positive and negative spikes around time zero, which are due to the non-resonant response of the solvent, the time profile can be well reproduced using a biexponential function with a rise time of 800 fs and a decay time of 2.6 ps. This rise time is consistent with the quenching time of LYen determined by fluorescence up-conversion. On the other hand, the very fast decay of the 580 nm transient absorption could be due to the geminate charge recombination or to a further reaction of $Trp^{\bullet+}$ such as a proton transfer.

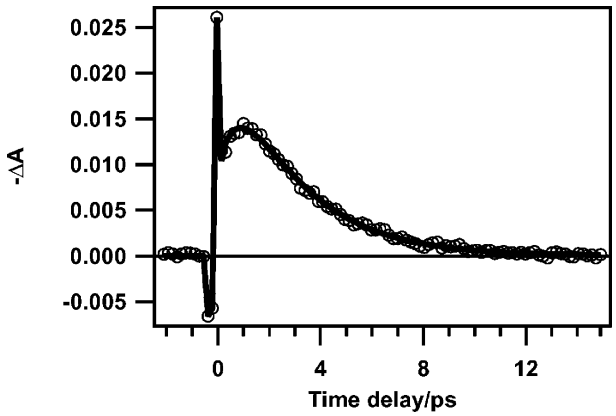

Fig. 9 Transient absorption kinetics at 580 nm of LYen in the presence of 40 mM Trp. The transient absorption is ascribed to $Trp^{\bullet+}$. Data points (open circles) were reproduced with a biexponential function (solid line).

Lucifer Yellow biocytin with avidin

To monitor the influence of a protein environment on the photophysics of Lucifer Yellow, the excited-state lifetime of LYbtn, a commercial construct in which the dye is coupled to biotin *via* a 13-atom spacer, was measured in the presence of avidin using TCSPC. Avidin is known for its very large affinity for biotin and can bind up to four such molecules.[69] The nanosecond fluorescence dynamics of LYbtn in a bulk solution is characterized by a single exponential decay of 7.0 ns (Fig. 10). In the presence of the protein, a further component of 1.0 ns accounting for 15–20% of the decay, depending on the number of occupied sites, was found (Table 5). The amplitude of the faster component rises with increasing LYbtn concentration. This component is already present at low LYbtn concentration, when only one binding site of avidin is occupied, suggesting that it arises from a direct interaction between the chromophore and the protein rather than from self-quenching of two neighbouring chromophores. A stoichiometric excess of LYbtn let the amplitude of the 1 ns component decrease again because of the presence of unbound fluorophore population, which contributes to the 7 ns component only. The origin of the 1 ns component upon binding to the protein is unknown and is under investigation. Nevertheless, these measurements suggest that, in spite of the long spacer in the LYbtn construct, Lucifer Yellow is able to sense the presence of the protein.

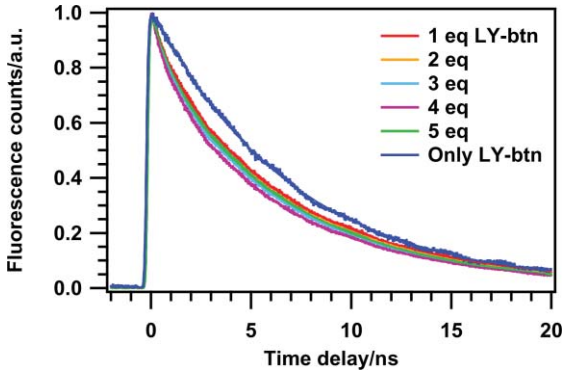

Fig. 10 Nanosecond fluorescence kinetics of an avidin sample titrated with 1 to 5 equivalents of LYbtn. The fluorescence decay of pure LYbtn in water is shown for comparison. The solid lines are the best fits.

Conclusions

This investigation has given a rather clear picture of the excited-state dynamics of LYen. After excitation at 400 nm and relaxation within a few ps, depending of the solvent, to the thermally equilibrated S_1 state, the molecule relaxes *via*

Table 5 Amplitudes a_i (accuracy: ±0.03) and lifetimes τ_i (accuracy: ±0.1 ns) obtained from the analysis of each TCSPC trace of Fig. 10; all four parameters were left free; eq.: equivalent(s)

c(Trp)	a_1	τ_1/ns	a_2	τ_2/ns
1 eq. LYbtn	0.87	6.8	0.13	1.0
2 eq. LYbtn	0.85	6.7	0.15	1.0
3 eq. LYbtn	0.83	6.6	0.17	1.0
4 eq. LYbtn	0.80	6.5	0.20	1.0
5 eq. LYbtn	0.86	6.6	0.14	1.0
Only LYbtn	1.00	7.0	—	—

fluorescence ($\tau_{rad} \approx$ 15–25 ns), intersystem crossing ($\tau_{ISC} \approx$ 25–35 ns), and, in protic solvents, in a large extent through reversible intermolecular proton transfer with the solvent ($\tau_{ESPT} \approx$ 10–12 ns).

Steady-state and fluorescence lifetime measurements demonstrated that LYen is an environment-sensitive probe able to discriminate between water, DMF, and DMSO and that heterogeneous microenvironments influence its early fluorescence dynamics. LYen fluorescence appears therefore well-suited as a probe of the local environment of proteins. Moreover, fluorescence quenching through nearby amino acid residues, especially tryptophan has also been shown to be operative. This effect might be at the origin of the decrease of the fluorescence lifetime of Lucifer Yellow biocytin in the presence of avidin. The influence of the protein on the ultrafast fluorescence dynamics is being investigated.

Acknowledgements

We would like to thank Professor Thomas Ward (University of Neuchâtel) for providing us with avidin and for discussion. This work was supported by the Fonds National Suisse de la Recherche Scientifique through project no. 200020-100014.

References

1 W. W. Stewart, Functional connections between cells as revealed by dye-coupling with a highly fluorescent naphthalimide tracer, *Cell*, 1978, **14**, 741–759.
2 W. W. Stewart, Lucifer dyes. Highly fluorescent dyes for biological tracing, *Nature*, 1981, **292**, 17–21.
3 P. Godement, J. Vanselow, S. Thanos and F. Bonhoeffer, A study in developing visual systems with a new method of staining neurones and their processes in fixed tissue, *Development*, 1987, **101**, 697–713.
4 N. Miro-Bernie, F. J. Sancho-Bielsa, C. Lopez-Garcia and J. Perez-Clausell, Retrograde transport of sodium selenite and intracellular injection of micro-ruby: A combined method to describe the morphology of zinc-rich neurons, *J. Neurosci. Methods*, 2003, **127**, 199–209.
5 J. F. Staiger, C. Masanneck, S. Bisler, A. Schleicher, W. Zuschratter and K. Zilles, Excitatory and inhibitory neurons express c-fos in barrel-related columns after exploration of a novel environment, *Neuroscience*, 2002, **109**, 687–699.
6 C. Peracchia, Direct communication between axons and sheath glial cells in crayfish, *Nature*, 1981, **290**, 597–598.
7 J. E. Contreras, H. A. Sanchez, E. A. Eugenin, D. Speidel, M. Theis, K. Willecke, F. F. Bukauskas, M. V. L. Bennett and J. C. Saez, Metabolic inhibition induces opening of unapposed connexin 43 gap junction hemichannels and reduces gap junctional communication in cortical astrocytes in culture, *Proc. Natl. Acad. Sci. USA*, 2002, **99**, 495–500.
8 W. J. Brown, J. Goodhouse and M. G. Farquhar, Mannose-6-phosphate receptors for lysosomal enzymes cycle between the golgi complex and endosomes, *J. Cell Biol.*, 1986, **103**, 1235–1247.
9 G. Drin, S. Cottin, E. Blanc, A. R. Rees and J. Temsamani, Studies on the internalization mechanism of cationic cell-penetrating peptides, *J. Biol. Chem.*, 2003, **278**, 31192–31201.
10 M. D. Taylor, J. R. Roberts, A. F. Hubbs, M. J. Reasor and J. M. Antonini, Quantitative image analysis of drug-induced lung fibrosis using laser scanning confocal microscopy, *Toxicol. Sci.*, 2002, **67**, 295–302.
11 J. M. Antonini, D. R. Hemenway and G. S. Davis, Quantitative image analysis of lung connective tissue in murine silicosis, *Exp. Lung Res.*, 2000, **26**, 71–88.
12 K. Yoneyama, Three-dimensional visualization and physiologic evaluation of bile canaliculi in the rat liver slice by confocal laser scanning microscopy, *Scanning*, 2001, **23**, 359–365.
13 M. Rocha and M. Sur, Rapid acquisition of dendritic spines by visual thalamic neurons after blockade of *N*-methyl-D-aspartate receptors, *Proc. Natl. Acad. Sci. USA*, 1995, **92**, 8026–8030.
14 M. J. Cabirol-Pol, A. Mizrahi, J. Simmers and P. Meyrand, Combining laser scanning confocal microscopy and electron microscopy to determine sites of synaptic contact between two identified neurons, *J. Neurosci. Methods*, 2000, **97**, 175–181.
15 A. Sommer, R. Gorges, G. M. Kostner, F. Paltauf and A. Hermetter, Sulfhydryl-selective fluorescence labeling of lipoprotein(a) reveals evidence for one single disulfide linkage between apoproteins(a) and B-100, *Biochemistry*, 1991, **30**, 11245–11249.
16 J. R. Archer, S. S. Badakere, M. G. Macey and M. A. Whelan, Use of lucifer yellow iodoacetamide in a flow cytometric assay to measure cell surface free thiol, *Biochem. Soc. Trans.*, 1995, **23**, 38.
17 J. P. Sumida, E. L. Forsythe and M. L. Pusey, Preparation and preliminary characterization of crystallizing fluorescent derivatives of chicken egg white lysozyme, *J. Cryst. Growth*, 2001, **232**, 308–316.
18 C. Kempf, M. R. Michel, U. Kohler and H. Koblet, A novel method for the detection of early events in cell-cell fusion of semliki forest virus infected cells growing in monolayer cultures, *Arch. Virol.*, 1987, **95**, 283–289.
19 B. C. Suh, S. K. Song, Y. K. Kim and K. T. Kim, Induction of cytosolic Ca2+ elevation mediated by Mas-7 occurs through membrane pore formation, *J. Biol. Chem.*, 1996, **271**, 32753–32759.
20 E. Picello, P. Pizzo and F. Di Virgilio, Chelation of cytoplasmic calcium increases plasma membrane permeability in murine macrophages, *J. Biol. Chem.*, 1990, **265**, 5635–5639.
21 A. Pardo, E. Martin, J. M. L. Poyato, J. J. Camacho, M. F. Brana and J. M. Castellano, Synthesis and photophysical properties of some *N*-substituted-1,8-naphthalimides, *J. Photochem. Photobiol. A*, 1987, **41**, 69–78.
22 P. Berci Filho, V. G. Toscano and M. J. Politi, Solvent-induced changes in the photophysical properties of *N*-alkylphthalimides, *J. Photochem. Photobiol. A*, 1988, **43**, 51–58.
23 A. Samanta, B. Ramachandram and G. Saroja, An investigation of the triplet state properties of 1,8-naphthalimide: A laser flash photolysis study, *J. Photochem. Photobiol. A*, 1996, **101**, 29–32.
24 P. Nemes, A. Demeter, L. Biczok, T. Berces, V. Wintgens, P. Valat and J. Kossanyi, Spectroscopic properties of aromatic dicarboximides part 4: *N*-alkyl- and *N*-cycloalkyl-substituted 1,2-naphthalimides, *J. Photochem. Photobiol. A*, 1998, **113**, 225–231.
25 D. Yuan and R. G. Brown, Enhanced nonradiative decay in aqueous solutions of aminonaphthalimide derivatives *via* water-cluster formation, *J. Phys. Chem. A*, 1997, **101**, 3461–3466.
26 A. P. de Silva, H. Q. N. Gunaratne, T. Gunnlaugsson, A. J. M. Huxley, C. P. McCoy, J. T. Rademacher and T. E. Rice, Signaling recognition events with fluorescent sensors and switches, *Chem. Rev.*, 1997, **97**, 1515–1566.
27 S. Saha and A. Samanta, Influence of the structure of the amino group and polarity of the medium on the photophysical behavior of 4-amino-1,8-naphthalimide derivatives, *J. Phys. Chem. A*, 2002, **106**, 4763–4771.
28 Y. Q. Gao and R. A. Marcus, Theoretical investigation of the directional electron transfer in 4-aminonaphthalimide compounds, *J. Phys. Chem. A*, 2002, **106**, 1956–1960.
29 J. A. Lee and P. A. G. Fortes, Labeling of the glycoprotein subunit of sodium-potassium atpase with fluorescent probes, *Biochemistry*, 1985, **24**, 322–330.
30 M. Sinev, P. Landsmann, E. Sineva, V. Ittah and E. Haas, Design consideration and probes for fluorescence resonance energy transfer studies, *Bioconjugate Chem.*, 2000, **11**, 352–362.
31 S. A. Kovalenko, R. Schanz, H. Hennig and N. P. Ernsting, Cooling dynamics of an optically excited molecular probe in solution from femtosecond broadband transient absorption spectroscopy, *J. Chem. Phys.*, 2001, **115**, 3256–3273.
32 D. Schwarzer, J. Troe and M. Zerezke, The role of local density in the collisional deactivation of vibrationally highly excited azulene in supercritical fluids, *J. Chem. Phys.*, 1997, **107**, 8380–8390.
33 A. Pigliucci and E. Vauthey, Vibrational relaxation dynamics of polyatomic molecules in solution, *Chimia*, 2003, **57**, 200–203.
34 M. L. Horng, J. A. Gardecki, A. Papazyan and M. Maroncelli, Subpicosecond measurements of polar solvation dynamics: Coumarin 153 revisited, *J. Phys. Chem.*, 1995, **99**, 17311–17337.
35 S. J. Rosenthal, X. Xie, M. Du and G. R. Fleming, Femtosecond solvation dynamics in acetonitrile: Observation of the inertial

contribution to the solvent response, *J. Chem. Phys.*, 1991, **95**, 4715–4718.
36 E. Vauthey, Picosecond transient grating study of the reorientation dynamics of nile red in different classes of solvent, *Chem. Phys. Lett.*, 1993, **216**, 530–536.
37 A. M. Williams, Y. Jiang and D. Ben-Amotz, Molecular reorientation dynamics and microscopic friction in liquids, *Chem. Phys.*, 1994, **180**, 119–129.
38 M. P. Pileni, Reverse micelles as microreactors, *J. Phys. Chem.*, 1993, **97**, 6961–6973.
39 M. Fischer and J. Georges, Use of thermal lens spectrometry for the investigation of dimerization equilibria of rhodamine 6g in water and aqueous micellar solutions, *Spectrochim. Acta, Part A*, 1997, **53A**, 1419–1430.
40 A. Morandeira, L. Engeli and E. Vauthey, Ultrafast charge recombination of photogenerated ion pairs to an electronic excited state, *J. Phys. Chem. A*, 2002, **106**, 4833–4837.
41 S. Pagès, B. Lang and E. Vauthey, Ultrafast spectroscopic investigation of the charge recombination dynamics of ion pairs formed upon highly exergonic bimolecular electron-transfer quenching: Looking for the normal region, *J. Phys. Chem. A*, 2004, **108**, 549–555.
42 P. Suppan, Solvatochromic shifts: The influence of the medium on the energy of electronic states, *J. Photochem. Photobiol. A*, 1990, **50**, 293–330.
43 A. Kapturkiewicz, J. Herbich, J. Karpiuk and J. Nowacki, Intramolecular radiative and radiationless charge recombination processes in donor-acceptor carbazole derivatives, *J. Phys. Chem. A*, 1997, **101**, 2332–2344.
44 S. J. Strickler and R. A. Berg, Relationship between absorption intensity and fluorescence lifetime of molecules, *J. Chem. Phys.*, 1962, **37**, 814–822.
45 B. Cohen and D. Huppert, Excited state proton-transfer reactions of coumarin 4 in protic solvents, *J. Phys. Chem. A*, 2001, **105**, 7157–7164.
46 N. Agmon, Elementary steps in excited-state proton transfer, *J. Phys. Chem. A*, 2005, **109**, 13–35.
47 H. T. Yu, W. J. Colucci, M. L. McLaughlin and M. D. Barkley, Fluorescence quenching in indoles by excited-state proton transfer, *J. Am. Chem. Soc.*, 1992, **114**, 8449–8454.
48 S. Das, A. Datta and K. Bhattacharyya, Deuterium isotope effect on 4-aminophthalimide in neat water and reverse micelles, *J. Phys. Chem. A*, 1997, **101**, 3299–3304.
49 R. Jimenez, G. R. Fleming, P. V. Kumar and M. Maroncelli, Femtosecond solvation dynamics of water, *Nature*, 1994, **369**, 471–473.
50 S. K. Pal, J. Peon, B. Bagchi and A. H. Zewail, Biological water: Femtosecond dynamics of macromolecular hydration, *J. Phys. Chem. B*, 2002, **106**, 12376–12395.
51 G. Onori and A. Santucci, IR investigations of water structure in aerosol OT reverse micellar aggregates, *J. Phys. Chem.*, 1993, **97**, 5430–5434.
52 D. J. Christopher, J. Yarwood, P. S. Belton and B. P. Hills, A fourier transform infrared study of water-head group interactions in reversed micelles containing sodium bis(2-ethylhexyl) sulfosuccinate (AOT), *J. Colloid Interface Sci.*, 1992, **152**, 465–472.
53 H. Hauser, G. Haering, A. Pande and P. L. Luisi, Interaction of water with sodium bis(2-ethyl-1-hexyl) sulfosuccinate in reversed micelles, *J. Phys. Chem.*, 1989, **93**, 7869–7876.
54 R. E. Riter, E. P. Undiks and N. E. Levinger, Impact of counterion on water motion in aerosol OT reverse micelles, *J. Am. Chem. Soc.*, 1998, **120**, 6062–6067.
55 M. Hasegawa, T. Sugimura, Y. Suzaki, Y. Shindo and A. Kitahara, Microviscosity in water pool of aerosol-OT reversed micelle determined with viscosity-sensitive fluorescence probe, auramine O and fluorescence depolarization of xanthene dyes, *J. Phys. Chem.*, 1994, **98**, 2120–2124.
56 S. K. Pal and A. H. Zewail, Dynamics of water in biological recognition, *Chem. Rev.*, 2004, **104**, 2099–2123.
57 G. Jones II, L. N. Lu, V. Vullev, D. J. Gosztola, S. R. Greenfield and M. R. Wasielewski, Photoinduced electron transfer for pyrenesulfonamide conjugates of tryptophan-containing peptides. Mitigation of fluoroprobe behavior in *N*-terminal labeling experiments, *Bioorg. Med. Chem. Lett.*, 1995, **5**, 2385–2390.
58 A. C. Vaiana, H. Neuweiler, A. Schulz, J. Wolfrum, M. Sauer and J. C. Smith, Fluorescence quenching of dyes by tryptophan: Interactions at atomic detail from combination of experiment and computer simulation, *J. Am. Chem. Soc.*, 2003, **125**, 14564–14572.
59 A. Harriman, Further comments on the redox potentials of tryptophan and tyrosine, *J. Phys. Chem.*, 1987, **91**, 6102–6104.
60 S. L. Murov, I. Carmichael and G. L. Hug, *Handbook of photochemistry*, Marcel Dekker, New York, 1993.
61 C. A. M. Seidel, A. Schulz and M. H. M. Sauer, Nucleobase-specific quenching of fluorescent dyes. 1. Nucleobase one-electron redox potentials and their correlation with static and dynamic quenching efficiencies, *J. Phys. Chem.*, 1996, **100**, 5541–5553.
62 F. D. Lewis, R. L. Letsinger and M. R. Wasielewski, Dynamics of photoinduced charge transfer and hole transport in synthetic DNA hairpins, *Acc. Chem. Res.*, 2001, **34**, 159–170.
63 G. Merenyi, J. Lind and X. Shen, Electron transfer from indoles, phenol and sulfite (SO_3^{2-}) to chlorine dioxide (ClO_2), *J. Phys. Chem.*, 1988, **92**, 134–137.
64 N. Marmé, J.-P. Knemeyer, M. Sauer and J. Wolfrum, Inter- and intramolecular fluorescence quenching of organic dyes by tryptophan, *Bioconjugate Chem.*, 2003, **14**, 1133–1139.
65 D. Zhong and A. H. Zewail, Femtosecond dynamics of flavoproteins: Charge separation and recombination in riboflavin (vitamin B2)-binding protein and in glucose oxidase enzyme, *Proc. Natl. Acad. Sci. USA*, 2001, **98**, 11867–11872.
66 J. E. Rogers and L. A. Kelly, Nucleic acid oxidation mediated by naphthalene and benzophenone imide and diimide derivatives: Consequences for DNA redox chemistry, *J. Am. Chem. Soc.*, 1999, **121**, 3854–3861.
67 J. E. Rogers, S. J. Weiss and L. A. Kelly, Photoprocesses of naphthalene imide and diimide derivatives in aqueous solutions of DNA, *J. Am. Chem. Soc.*, 2000, **122**, 427–436.
68 I. A. Shkrob, M. C. Sauer, Jr, A. D. Liu, R. A. Crowell and A. D. Trifunac, Reactions of photoexcited aromatic radical cations with polar solvents, *J. Phys. Chem. A*, 1998, **102**, 4976–4989.
69 Avidin-biotin technology, in *Methods in Enzymology*, ed. M. Wilchek and E. A. Bayer, Academic Press, San Diego, 1990, vol. 184, p. 746.